

On the Charge Separation Effect in Relativistic Heavy Ion Collisions

Jinfeng Liao ¹, Volker Koch ¹, and Adam Bzdak ^{1,2}

¹*Nuclear Science Division, Lawrence Berkeley National Laboratory,
MS70R0319, 1 Cyclotron Road, Berkeley, California 94720, USA.*

²*Institute of Nuclear Physics, Polish Academy of Sciences,
Radzikowskiego 152, 31-342 Krakow, Poland.*

Abstract

In this paper, we discuss alternative means of measuring the possible presence of local parity violation in relativistic heavy ion collisions. We focus on the phenomenon of charge separation and introduce the charged dipole vector \hat{Q}_1^c , which will measure the charge separation on an event-by-event basis. Using Monte Carlo events, we demonstrate the method and its discriminating power. In particular we show that such an analysis will reveal the strength of charge separation effect and its azimuthal correlation with the reaction plane. We further show that our proposed method may be able to distinguish between the actual charge separation effect and effects due to certain two particle correlations. The connection to present measurements based on particle correlations is discussed.

Keywords: charge separation, Chiral Magnetic Effect, topological objects

PACS numbers: 25.75.-q, 12.38.Mh, 25.75.Gz, 11.30.Er

I. INTRODUCTION

Topological objects in Quantum Chromodynamics(QCD) (and generally in non-Abelian gauge theories) have attracted persistent theoretical interests and are important in many aspects [1]. For example, instantons are known to be responsible for various properties of the QCD vacuum, such as spontaneous breaking of chiral symmetry and the $U_A(1)$ anomaly (see e.g. [2][3]). Magnetic monopoles, on the other hand, are speculated to be present in the QCD vacuum in a Bose-condensed form which then enforce the color confinement, known as the dual superconductor scenario for QCD confinement which is strongly supported by evidences from lattice QCD (see e.g. [4][5]). Alternatively vortices are also believed to describe the chromo-electric flux configuration (i.e. flux tube) between a quark-anti-quark pair in the QCD vacuum which in turn gives rise to the confining linear potential (see e.g. reviews in [5][6]). Some of these objects, such as monopoles [7] and flux tubes [8], may also be important degrees of freedom in the hot and deconfined QCD matter close to the transition temperature T_c , and may be responsible for the observed properties of the so called strongly coupled quark-gluon plasma [9]. Certain phenomenological consequences of such topological objects for relativistic heavy ion collisions have been studied in [10].

A particularly interesting suggestion by Kharzeev and collaborators [11–16] on the direct manifestation of effects from topological objects is the possible occurrence of \mathcal{P} - and \mathcal{CP} -odd (local) domains due to the so-called sphaleron transitions in the hot dense QCD matter created in the relativistic heavy ion collisions. In particular, the so called Chiral Magnetic Effect(CME)[13] predicts that in the presences of the strong external (electrodynamic) magnetic field at the early stage after a (non-central) collision sphaleron transitions induce a separation of charges along the direction of the magnetic field. Since the external magnetic field is perpendicular to the reaction plane defined by the impact parameter and the beam axis, one expects an out-of-plane charge separation. As a result positive charges are expected to preferentially go in one (out-of-plane) direction and negative charges in the opposite (out-of-plane) direction. In a given event, this charge separation results in a momentum space electric dipole which breaks parity. However, the dipole moment will be, with equal probability, parallel or anti-parallel to the magnetic field depending whether the Chiral Magnetic Effect is caused by a sphaleron or anti-sphaleron transition. Consequently, the expectation value of the dipole or, more precisely, of the scalar product of the dipole

and the magnetic field, will vanish.

For the aforementioned reasons the CME will *not* give rise to a non-vanishing expectation value of a \mathcal{P} -odd observable. However, the fact that parity is broken event-by-event should be reflected in the variance of a \mathcal{P} -odd observable, which, however is a \mathcal{P} -even observable. Therefore, other, non-parity violating processes may contribute which need to be well understood.

Very recently the STAR collaboration has announced the first experimental evidence of a possible local parity violation phenomenon at the Brookhaven's Relativistic Heavy Ion Collider(RHIC) [17]. STAR has measured the differences between the in-plane-projected and out-of-plane-projected 2-particle azimuthal correlations for both same-charge pairs and opposite-charge pairs, as proposed by Voloshin in [18]. The data indeed show very interesting charged-pair correlation patterns that depend on the charges (same/opposite), reaction plane (in-plane/out-of-plane), average p_t of pairs, and colliding nuclei (Au/Cu). At first sight, some features of the data appear to be consistent with what has been expected from the local parity violation phenomenon. However, as shown in Ref.[19], certain aspects of the data appear to be puzzling at present: contrary to expectations from the Chiral Magnetic effect, the same-sign pairs show a negative in-plane instead of a positive out-of-plane correlation. Consequently, an interpretation of the data in terms of local-parity-violation would require a nearly exact cancellation for all centralities of correlations due to the Chiral Magnetic Effect and those due to ordinary correlations. In addition, further studies have proposed alternative contributions to the observed signals [20, 21], and various possible consequences related to the local parity violation [22] and the Chiral Magnetic Effect [23, 24] have been recently discussed. At present, therefore, the existence of local parity violation in heavy ion collisions has not yet been definitively established and further detailed and more differential analysis of the current observable as well as the development of alternative observables are necessary.

The purpose of this paper is to propose and study in detail an alternative observable which specifically measures the charge separation predicted by the CME. To this end we generally investigate the charge separation effect as an intrinsic charge-dependent particle azimuthal distribution, and propose a way of measuring the magnitude of the charge separation effect and its orientation relative to the reaction plane. The orientation, if experimentally measured, will be essential for an evaluation of the proposed local parity violation and CME

interpretation.

In the following, we will first introduce an intrinsic charge-dependent distribution representing the charge separation effect. We will then propose the charged dipole vector \hat{Q}_1^c analysis method and demonstrate its discriminating power by applying it to Monte Carlo events. We will also present a detailed study of the impact of certain two-particle correlations which may contribute to charge separation and cause ambiguity in the interpretation of the present STAR data. We will show that even with in the presence of these background correlations the measurement of \hat{Q}_1^c together with the correlations proposed by STAR may be able to unravel the charge separation, its orientation and the various sources contributing to it.

II. THE CHARGE SEPARATION EFFECT

Let us begin by specifying what we mean by the charge separation effect in this paper. Consider the distribution of final state hadrons in the transverse momentum space as schematically shown in the Fig.1. If the “center” of the positive charges happens to be different from that of the negative charges, then there is a separation between two types of charges which may be quantified by an “electric dipole moment” in the transverse momentum space. Such a separation may arise either simply from statistical fluctuations or may be due to specific dynamics, such as the Chiral Magnetic Effect. The later case is

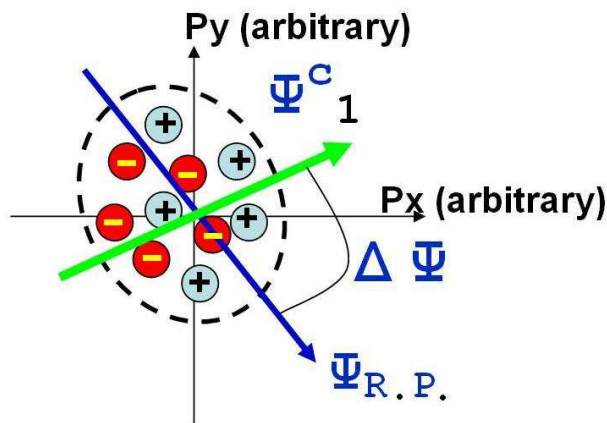


FIG. 1: A schematic demonstration of the proposed simultaneous analysis of \hat{Q}_1^c and \hat{Q}_2 vectors in the same event.

best discussed in the *intrinsic* frame, i.e. the frame defined by the direction of the reaction plane $\Psi_{R.P.}$. There, we can define an *intrinsic* charge-dependent single particle azimuthal distribution, which, besides a possible momentum-space electric dipole moment, also allows for the presence of elliptic flow.

$$f_\chi(\phi, q) \propto 1 + 2v_2 \cos(2\phi - 2\Psi_{R.P.}) + 2q\chi d_1 \cos(\phi - \Psi_{C.S.}) \quad (1)$$

Here q and ϕ represent the charge and the azimuthal angle of a particle, respectively. The parameters v_2 and d_1 quantify the elliptic flow and the charge separation effect, while $\Psi_{C.S.}$ specifies the azimuthal orientation of the electric-dipole (see Fig.1) and $\Psi_{R.P.}$ the direction of the reaction plane. It is important to notice that an additional random variable $\chi = \pm 1$ is introduced. This accounts for the fact that in a given event we may have sphaleron or anti-sphaleron transitions resulting in charge separation parallel or anti-parallel to the magnetic field. Consequently the sampling over all events with a given reaction plane angle, $\Psi_{R.P.}$, corresponds to averaging the intrinsic distribution f_χ over χ , namely $f = \langle f_\chi \rangle_\chi \propto 1 + 2v_2 \cos(2\phi - 2\Psi_{R.P.})$. Physically speaking this means that the charge separation (or electric dipole, being \mathcal{P} -odd) flips and averages out to zero, thus causing the expectation value of any parity-odd operator to vanish. However, since $\langle \chi^2 \rangle = 1$ the presence of an event-by-event electric dipole may be observable in the *variance* of a parity-odd operator.

Provided an accurate identification of the reaction plane is possible one may also redefine the angles by setting $\Psi_{R.P.} = 0$ and replacing $\Psi_{C.S.}$ by $\Delta\Psi_{C.S.} \equiv \Psi_{C.S.} - \Psi_{R.P.}$ in Eq.(1). For $\Delta\Psi_{C.S.} = \pi/2$ the charge separation term takes the form of $d \sin(\phi)$ as expected from the Chiral Magnetic Effect [16–18].

For measurements related to heavy ion collisions one may reasonably assume particle charges to be $|q| = 1$ which is the case for almost all charged particles e.g. charged pions and kaons, protons, etc. We also emphasize that the above distributions does *not* contain a directed flow term for either type of charges. Finally one may also consider a p_t -differential formulation of the charge separation effect or charge separation effects associated with higher harmonics in the azimuthal angle ϕ .

Let us next discuss how the above defined charge-dependent intrinsic single-particle distribution contributes to the charged particle correlations recently measured by the STAR collaboration in [17]. Before doing so we note that there will likely be additional contributions from two- and multi-particle correlations which we will not consider in this Section.

The STAR collaboration has measured charge dependent two- and three-particle correlations [17]. Specifically they considered

(i) The two-particle correlation $\langle \cos(\phi_i - \phi_j) \rangle$ for same-charge pairs ($++ / --$) and opposite-charge pairs ($+-$). The contribution to this correlator due to the charge-dependent intrinsic single-particle distribution, Eq.(1) is:

$$\langle \cos(\phi_i - \phi_j) \rangle_{++/--} = d_1^2 \quad (2)$$

$$\langle \cos(\phi_i - \phi_j) \rangle_{+-} = -d_1^2 \quad (3)$$

(ii) The three-particle correlation $\langle \cos(\phi_i + \phi_j - 2\phi_k) \rangle$ for same-charge pairs ($i, j = ++ / --$) and opposite-charge pairs ($i, j = +-$) with the third particle, denoted by index k , having any charge. The contribution to these correlators due to the distribution, Eq.(1) turns out to be

$$\langle \cos(\phi_i + \phi_j - 2\phi_k) \rangle_{++/--, k-any} = v_2 d_1^2 \cos(2 \Delta \Psi_{C.S.}) \quad (4)$$

$$\langle \cos(\phi_i + \phi_j - 2\phi_k) \rangle_{+-, k-any} = -v_2 d_1^2 \cos(2 \Delta \Psi_{C.S.}) \quad (5)$$

where “k-any” indicates that the charge of the 3-rd particle may assume any value/sign. The STAR collaboration has demonstrated [17] that the above three particle correlator is dominated by the reaction plane dependent two-particles correlation function $\langle \cos(\phi_i + \phi_j - 2\Psi_{R.P.}) \rangle$ and within errors they have found that

$$\langle \cos(\phi_i + \phi_j - 2\phi_k) \rangle = v_2 \langle \cos(\phi_i + \phi_j - 2\Psi_{R.P.}) \rangle \quad (6)$$

Based on the distribution Eq.(1) we find the same relation between these correlation functions, since the reaction-plane dependent two-particle correlation is given by

$$\langle \cos(\phi_i + \phi_j - 2\Psi_{R.P.}) \rangle_{++/--} = d_1^2 \cos(2 \Delta \Psi_{C.S.}) \quad (7)$$

for same-charge pairs, and

$$\langle \cos(\phi_i + \phi_j - 2\Psi_{R.P.}) \rangle_{+-} = -d_1^2 \cos(2 \Delta \Psi_{C.S.}) \quad (8)$$

for opposite-charge pairs.

The proposed Chiral Magnetic Effect corresponds to $\Delta \Psi_{C.S.} = \frac{\pi}{2}$. In this case

$$\langle \cos(\phi_i + \phi_j - 2\Psi_{R.P.}) \rangle_{++/--} = -d_1^2 < 0, \quad (9)$$

$$\langle \cos(\phi_i - \phi_j) \rangle_{++/--} = +d_1^2 > 0. \quad (10)$$

Thus, the two correlation functions are expected to be equal in magnitude with *opposite* sign. The STAR measurement, on the other hand finds them approximately equal in magnitude but with the *same* (negative) sign. This discrepancy, which is discussed in detail in [19], needs to be understood before any definitive conclusions about a possible charge separation effect can be drawn. One aspect is the effect of higher order correlations, which we have so far ignored.

In the following Section we present an alternative observable which is sensitive to a potential charge separation effect. As we will discuss in detail, this observable will take into account additional correlations beyond those considered by STAR and thus may help to clarify the present situation.

III. MEASUREMENT OF CHARGE SEPARATION BY \hat{Q}_1^c ANALYSIS

In this Section we will present a method to directly measure the intrinsic charge-dependent distribution in Eq.(1). We propose to measure the charged dipole moment vector \hat{Q}_1^c of the final-state hadron distribution in the transverse momentum space. The magnitude Q_1^c and azimuthal angle Ψ_1^c of this vector can be determined in a given event by the following:

$$\begin{aligned} Q_1^c \cos \Psi_1^c &\equiv \sum_i q_i \cos \phi_i \\ Q_1^c \sin \Psi_1^c &\equiv \sum_i q_i \sin \phi_i \end{aligned} \quad (11)$$

where the summation is over all charged particles in the event with q_i and ϕ_i the electric charge¹ and azimuthal angle of each particle. This method is in close analogy to the \hat{Q}_1 and \hat{Q}_2 vector analysis used for directed and elliptic flow (see e.g. [25]). In particular the elliptic flow and the reaction plane orientation can be determined via the \hat{Q}_2 vector (with magnitude Q_2 and azimuthal angle Ψ_2) as:

$$\begin{aligned} Q_2 \cos 2\Psi_2 &\equiv \sum_i \cos 2\phi_i \\ Q_2 \sin 2\Psi_2 &\equiv \sum_i \sin 2\phi_i \end{aligned} \quad (12)$$

¹ As already mentioned, one may reasonably assume $|q_i| = 1$.

We emphasize that contrary to \hat{Q}_2 the charge dipole vector, \hat{Q}_1^c , incorporates the *electric charge* q_i of the particles². The angles Ψ_1^c and Ψ_2 are determined event-by-event from a finite number of particles and are not to be confused with the idealized expectations $\Psi_{C.S.}$ and $\Psi_{R.P.}$, although they should become identical in the limit of infinite multiplicity.

With both the magnitude Q_1^c and the azimuthal angle Ψ_1^c determined on an event-by-event basis, important information about the underlying physics can be revealed.³ In particular, the event-by-event distribution of the magnitude Q_1^c may indicate if there is a physical charge separation effect beyond pure statistical fluctuations. Furthermore, the relative distribution of the angle Ψ_1^c with respect to the reaction plane determined in the same event (e.g. via the \hat{Q}_2 analysis) can show to which extent the charge separation is correlated with the reaction plane with a specific angle $\Delta\Psi_{C.S.} = \Psi_{C.S.} - \Psi_{R.P.}$ (see Fig.1).

Next let us investigate the discriminating power of the proposed \hat{Q}_1^c analysis for a potential charge separation effect. To this end we employ Monte Carlo sampling to generate an ensemble of final state hadrons with equal numbers of π^+ and π^- . For each particle we sample an azimuthal angle ϕ_i of its transverse momentum \vec{p}_t . We do not sample the magnitude of the transverse momentum, p_t , as the \hat{Q}_1^c analysis defined in Eq.(11) involves only the angle ϕ_i ⁴.

To mimic an event that may have elliptic flow and a possible charge separation effect, we sample the azimuthal angles for $N_+ = 200$ π^+ and $N_- = 200$ π^- according to the intrinsic distribution in Eq.(1)^{5 6}. The sampling parameter v_2 specifies the magnitude of the elliptic flow and $\Psi_{R.P.}$ the orientation of the reaction plane, which is randomly chosen in each event. The parameters d_1 and $\Psi_{C.S.}$ specify the magnitude of charge separation effect and the orientation of the charged dipole, respectively. Finally for each event we randomly

² Mathematical details regarding the observable \hat{Q}_1^c can be found in the Appendix.

³ After the completion of the present work, we became aware of the recent PHENIX efforts [27] to measure the distribution of the difference of $\sum \sin(\phi_i)$ between plus and minus charges. This is related to the quantity $Q_1^c \sin \Psi_1^c$, which is part of the full information that can be extracted by the \hat{Q}_1^c analysis.

⁴ One may actually assign p_t -dependent weight factor in the definition of \hat{Q}_1^c to maximize manifestation of the desired physical effect, as has been done in the v_2 analysis (see e.g. [25]).

⁵ To be more realistic one shall allow for fluctuations of the particle numbers, N_+ and N_- , within a selected multiplicity window. These additional sources of background statistical fluctuations bring in negligible broadening of the \hat{Q}_1^c magnitude distribution curves in Fig.2 as we have verified numerically with up to $\pm 20\%$ fluctuations independently for N_+ and N_- .

⁶ We emphasize again that in such sampling, *no* directed flow effect will be generated and only pure statistic fluctuations will contribute in the usual \hat{Q}_1 analysis.

pick the sign of the parameter $\chi = \pm 1$.

In order to investigate different physical situations we consider a variety of cases as follows:

Case-Ia with $d_1 = 0$ and $v_2 = 0$, and **Case-Ib** with $d_1 = 0$ but $v_2 \neq 0$. In both cases the charge separation may arise only from statistical fluctuations with or without the presence of elliptic flow;

Case-II with $d_1 \neq 0$ but $v_2 = 0$. Here we allow for an explicit charge separation in addition to statistical fluctuations but do not consider any explicit elliptic flow;

Case-IIIa with $d_1 \neq 0$ and $v_2 \neq 0$ but with the two orientations $\Psi_{C.S.}$ and $\Psi_{R.P.}$ randomly assigned in each event, representing a situation where both charge separation and elliptic flow are present but *not* correlated in the azimuth;

Case-IIIb with $d_1 \neq 0$ and $v_2 \neq 0$ and with the two orientations $\Psi_{C.S.}$ and $\Psi_{R.P.}$ always parallel in each event;

Case-IIIc with $d_1 \neq 0$ and $v_2 \neq 0$ and with the two orientations $\Psi_{C.S.}$ and $\Psi_{R.P.}$ always perpendicular in each event;

Case-IIId with $d_1 \neq 0$ and $v_2 \neq 0$ and with the two orientations $\Psi_{C.S.}$ and $\Psi_{R.P.}$ always $\frac{\pi}{4}$ apart in each event.

A comparison between the various cases will allow us to test the ability of the proposed analysis to discriminate between the various physical scenarios.

For each of the above cases we sample 100 million events. For each event we perform the \hat{Q}_2 and \hat{Q}_1^c analyses and extract the values Q_2, Ψ_2 and Q_1^c, Ψ_1^c . The resulting distributions of the magnitude Q_1^c and the angle Ψ_1^c for the charged dipole vector \hat{Q}_1^c will be presented and discussed in the following subsections.

A. The Magnitude Distribution

The Q_1^c magnitude distributions (normalized to unity) for the various aforementioned cases are shown in Fig.2. We have chosen the following values for the sampling parameters: For the cases with non-vanishing dipole moment, Case-II and Case-IIIa,b,c,d, we have used $d_1 = 0.05$. For the cases with non-vanishing elliptic flow, Case-Ib and Case-IIIa,b,c,d, we allowed for two values of elliptic flow parameter $v_2 = 0.1$ and $v_2 = 0.05$ in each case. Therefore, overall there are *twelve* curves in the plot: interestingly, they all fall into only two

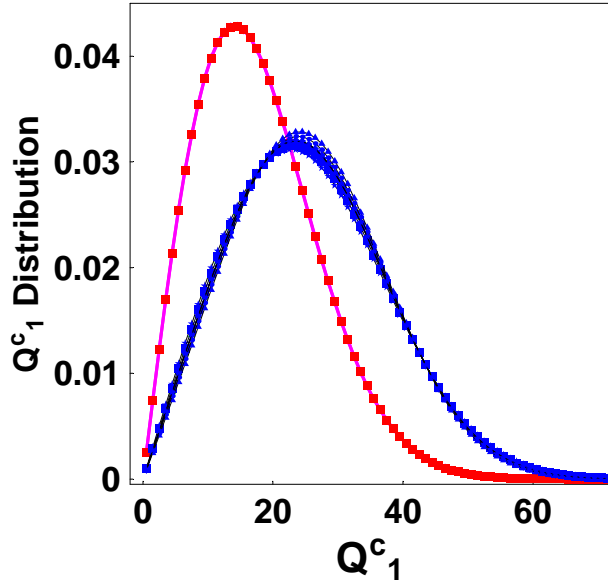


FIG. 2: The Q_1^c magnitude distribution extracted from sampled events for the various cases. The curves for Case-Ia (red) and for Case-Ib with two values of v_2 (magenta) appear on top of each other at the left, while the curves for Case-II(green) and for Case-IIIa,b,c,d with two values of v_2 for each(blue) appear on top of each other at the right (see text for details).

groups. One group includes all the curves corresponding to the cases with $d_1 = 0$ (left set of curves in Fig.2) and the other corresponds to all cases with finite dipole moment, $d_1 = 0.05$, irrespective of the presence and strength of elliptic flow.

From these result we may conclude the following: (a) the Q_1^c magnitude distribution is very sensitive to the physical charge separation effect represented by d_1 , but rather unaffected by the elliptic flow v_2 ; (b) the left curve(s) in Fig.2 represents the pure statistical fluctuation, and any deviation of the measured distribution from this curve would contain information about the physical charge separation effect. Experimentally the reference curve from statistical fluctuation can be obtained by randomly re-assigning the charges of the particles in each event. We have verified with our sampling, that the analysis after charge-reshuffling shifts all the curves to the statistical ones, denoted as Case Ia and Ib in Fig.2.

B. The Angular Distribution

We next turn to the angular distribution. Since any experiment samples over all directions of the reaction plane the only experimental accessible information is the relative angle, $\Delta\Psi = \Psi_1^c - \Psi_2$, between the direction of the charge dipole, Ψ_1^c , and that of the reaction plane, or more precisely, the elliptic flow, Ψ_2 .

We focus on the four cases Case-IIIa,b,c,d, where both the elliptic flow and the charge separation effects are present. For studies in the present subsection, we set $v_2 = 0.1$ and $d_1 = 0.05$ in the sampling. For each sampled event we then extract the angles Ψ_1^c and Ψ_2 from each event and calculate their difference $\Delta\Psi = \Psi_1^c - \Psi_2$. Since the angle Ψ_2 (essentially the reaction plane orientation) is defined modulus π , $\Delta\Psi$ is equivalent to $\Delta\Psi \pm \pi$ and we may always transform $\Delta\Psi$ to be in the interval $\Delta\Psi \in [-\pi/2, \pi/2]$ ⁷. Furthermore, what matters most for our discussion is the distinction between the in-plane and the out-of-plane orientations. Thus it is sufficient to know the absolute value of $\Delta\Psi$, i.e. $|\Delta\Psi| \in [0, \pi/2]$.

The resulting $|\Delta\Psi|$ distributions for the Cases IIIa,b,c,d are shown in Fig.3(left). They clearly exhibit distinctive patterns for the various cases. Out of the four cases, the Case-IIIa serves as a background since in this case the orientations of the elliptic flow and the dipole are *uncorrelated*⁸. Any deviation from the Case-IIIa $|\Delta\Psi|$ distribution indicates an azimuthal correlation between the dipole and the elliptic flow. This background may be removed by subtracting the results from Case-IIIa in our model. Such subtracted $|\Delta\Psi|$ distributions for the Case-IIIb,c,d are shown in Fig.3(right) for comparison.

The curve for Case-IIIb, where the orientations for the elliptic flow and charge separation effects are taken to be parallel, $\Psi_{C.S.} = \Psi_{R.P.}$, shows a maximum at $|\Delta\Psi| = 0$ (in plane) and a rapid decrease toward $|\Delta\Psi| = \pi/2$ (out-of-plane). Thus the dipole \hat{Q}_1^c is predominantly

⁷ In addition, the direction of the electric dipole moment is only known modulo π due to the random factor χ in Eq.(1) representing the equal likelihood of sphalerons and anti-sphalerons.

⁸ We note that even for the Case-IIIa where there is no a prior correlation in the sampling, the distribution is not entirely flat but slightly favors a smaller angular separation between Ψ_1^c and Ψ_2 . This is not surprising as both \hat{Q}_1^c and \hat{Q}_2 are determined from the same set of particles in a given event. Given the probability distribution, Eq.(1), it is clear that for any angular sampling parameters $\Psi_{C.S.}$ and $\Psi_{R.P.}$ the maximum of the probability distribution is located at certain angle Ψ_{max} (and $\Psi_{max} + \pi$ for the opposite charge) between the two. As a result both angles, Ψ_1^c and Ψ_2 , extracted from the sampled events tend to slightly align with the maximal angle Ψ_{max} . In an actual data analysis, this background Case-IIIa angular distribution can be well approximated by the angular distribution from pure statistical background obtainable via the previously mentioned charge-resuffling, as we have verified with our sampling.

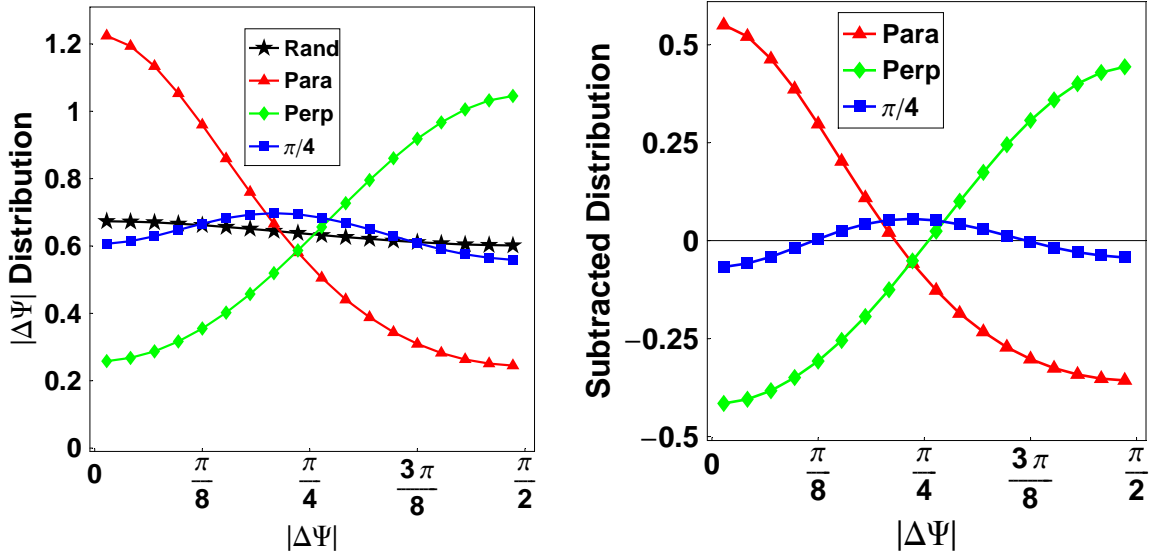


FIG. 3: (left) The distributions of the relative azimuthal angle $|\Delta\Psi|$ between the charged dipole vector \hat{Q}_1^c and the reaction plane for Case-IIIa (black star), b (red triangle), c (green diamond), d (blue box). (right) The subtracted distributions (i.e. the difference with respect to the Case-IIIa distribution) for Case-IIIb (red triangle), Case-IIIc (green diamond), and Case-IIId (blue box) respectively. (See text for more details).

oriented in-plane. The curve for Case-IIIc, where the orientations for the elliptic flow and charge separation effects are taken to be perpendicular, shows exactly the opposite. Finally the curve for Case-IIId, where the orientations for the elliptic flow and charge separation effects are sampled to be $\pi/4$ apart from each other, features a maximum around $|\Delta\Psi| = \pi/4$ and a decrease toward both ends. The effect, however is not as prominent as in the previous cases and it may be more difficult to separate it from the background Case-IIIa. For these scenarios we have also varied values of both v_2 and d_1 in our sampling and found the patterns to be qualitatively the same (see Section IV for details).

From these studies, one can conclude that by simultaneously measuring the orientations of \hat{Q}_1^c and \hat{Q}_2 and examining their angular difference distribution, the azimuthal correlation between the two physical effects may be extracted.

C. An Alternative Measurement of Relative Orientation

While measuring the relative orientation distribution as discussed in the previous subsection contains the “full” information, it is experimentally rather demanding as it requires determination of reaction plane in each event. There is an alternative way to determine whether the charged dipole \hat{Q}_1^c is closer to the in-plane or out-of-plane direction without the need of reaction plane. The idea is to measure the correlation function $\langle \cos(2\Delta\Psi) \rangle = \langle \cos(2\Psi_{C.S.} - 2\Psi_{R.P.}) \rangle$,⁹ which in a sense represents the “elliptic anisotropy” of \hat{Q}_1^c . By using the definitions in Eqs.(11,12), one obtains

$$\langle \cos(2\Delta\Psi) \rangle = \left\langle \frac{N_{ch} + 2\{i, j\}_1^c + \{i, j\}_2 + \{i, j; k\}^c}{[N_{ch} + \{i, j\}_1^c] \cdot [N_{ch} + \{i, j\}_2]^{1/2}} \right\rangle \quad (13)$$

with the two- and three- particle correlations defined as

$$\begin{aligned} \{i, j\}_1^c &\equiv \sum_{i \neq j} q_i q_j \cos(\phi_i - \phi_j) \\ \{i, j\}_2 &\equiv \sum_{i \neq j} \cos 2(\phi_i - \phi_j) \\ \{i, j; k\}^c &\equiv \sum_{i \neq j \neq k} q_i q_j \cos(\phi_i + \phi_j - 2\phi_k) \end{aligned} \quad (14)$$

(see the Appendix A for details).

If the observable $\langle \cos(2\Delta\Psi) \rangle$ is measured to be unambiguously negative/positive then the charge separation is closer to out-of-plane/in-plane. If it is however consistent with zero within errors, then the situation is unclear. An ideal Chiral Magnetic Effect without any other effect and without statistical fluctuations would predict $\langle \cos(2\Delta\Psi) \rangle = -1$. As will be discussed in the next Section, however, statistical fluctuations and additional two-particle correlations may lead to sizable corrections.

Let us finally point out that the correlation function, Eq.(13), in principle involves particle correlations to all orders, since it represents an average of a ratio. In addition, the correlators appearing in the denominator, in particular $\{i, j\}_2$, is of the same magnitude as N_{ch} , which makes an expansion of the denominator unreliable. Consequently, the correlation function, Eq.(13), has to be measured in its entirety and represents a different measurement than that

⁹ A similar correlation between the directed flow and elliptic flow was proposed by Poskanzer and Voloshin in [26] to determine their relative orientation.

of the individual terms, which has been already carried out by the STAR collaboration. A dedicated measurement is thus important and urgently called for.

IV. DISENTANGLING CHARGE SEPARATION AND TWO-PARTICLE CORRELATIONS

In this Section we focus on the influence of certain two-particle correlations on both the observables proposed in the present paper and the correlations measured by STAR. As has been shown in [19], the present STAR data indicates the existence of at least two types of correlations (beyond the possible correlations predicted by the Chiral Magnetic Effect): same-charge pair back-to-back correlations (mostly in-plane), and opposite-charge pair same-side correlations (about equally in-plane and out-of-plane). It is therefore important to study the robustness of various observables against such “background correlations”, and in particular to evaluate the prospects of disentangling a physical dipole charge separation from those background correlations. Physically speaking, there are a number of potential sources that may induce such two-particle correlations, such as clusters, momentum and/or local charge conservation [20][21], or even chiral magnetic spiral effect [24].

In order to study correlation effects we introduce correlations on top of our previous sampling based on single particle distribution in Eq.(1). In particular we test the two types indicated by data, i.e.: (a) same-charge pair back-to-back correlation (**SCBB**), which we implement by randomly selecting a small fraction of same-charge pairs and sampling them according to $|\phi_1 - \phi_2| > \pi/2$; (b) opposite-charge pair same-side correlation (**OCSS**), which we implement by randomly selecting a small fraction of opposite-charge pairs and sampling them according to $|\phi_1 - \phi_2| < \pi/2$. At the same time we ensure the single particle distribution remains unchanged.¹⁰ In the following we discuss various situations with different choices for the strength of the dipole charge separation and the correlations. For all studies in this Section we set $v_2 = 0.1$ and generate 10 million events for each case.

¹⁰ The precise procedure we used here is the following: when sampling each particle (say a plus charge) we trigger the correlation with probability 0.4 and once triggered we correlate it with the preceding plus/minus charge for SCBB/OCSS correlations by sampling its angle according to both the single particle distribution and the constraint from correlation. We have studied different implementations (which essentially imply different approximations to the desired correlations) and found that our conclusions are not changed.

A. Test-I

In Test-I, we consider a setting with relatively “large” out-of-plane dipole and small correlations and study four cases:

Case-IIIc (previously studied) with dipole $d_1 = 0.05$ and $|\Delta\Psi| = \pi/2$ in the sampling;

Case-IIIc-(α) with the same dipole as in Case-IIIc, plus SCBB correlation at a fraction $f_{SCBB} = 0.4\%$ of all same-charge pairs ;

Case-IIIc-(β) with the same dipole as in Case-IIIc, plus OCSS correlation at a fraction $f_{OCSS} = 0.4\%$ of all opposite-charge pairs ;

Case-IIIc-(γ) with the same dipole as in Case-IIIc, plus both SCBB and OCSS correlations at the same fraction of $f_{SCBB} = f_{OCSS} = 0.4\%$.

The results for Q_1^c and $|\Delta\Psi|$ distributions are shown in Fig.4 and the various measured observables ¹¹ are reported in Table.I. From these results one can see that:

- (1) Both types of correlations shift the Q_1^c distribution towards smaller values, i.e. they *suppress* the charge separation;
- (2) The $|\Delta\Psi|$ distribution, on the other hand, is quite robust in the present setting and maintains a clear pattern characteristic of an out-of-plane charge separation in all four cases. However, the correlations lead to a slight flattening of the distributions.
- (3) Correspondingly, the observable $\langle \cos(2\Delta\Psi) \rangle$ remains negative for all cases, with its absolute value slightly reduced by both types of correlations;
- (4) The observable $\langle \cos(\phi_i + \phi_j - 2\phi_k) \rangle$ remains negative for same-charge pairs and positive for opposite-charge pairs;
- (5) The observable $\langle \cos(\phi_i - \phi_j) \rangle$ has completely different sign patterns in the four cases, and appears to be a sensitive diagnostic for different types of correlations;
- (6) The Case-IIIc-(γ) (see last column in Table.I), where the dipole coexists with both SCBB and OCSS correlations, is the only one which shows a sign patterns for all four measured charge correlations that is qualitatively similar to the STAR data.¹²

These results can be partly understood as follows: the physical dipole separates positive

¹¹ The definitions and interrelations of these observables can be found in the Appendix.

¹² One could imagine that tuning the strength of each of the three components may provide a reasonable fit to the presently available STAR data. Given the rather schematic correlations employed in this study, the value of such an exercise is, however, rather limited.

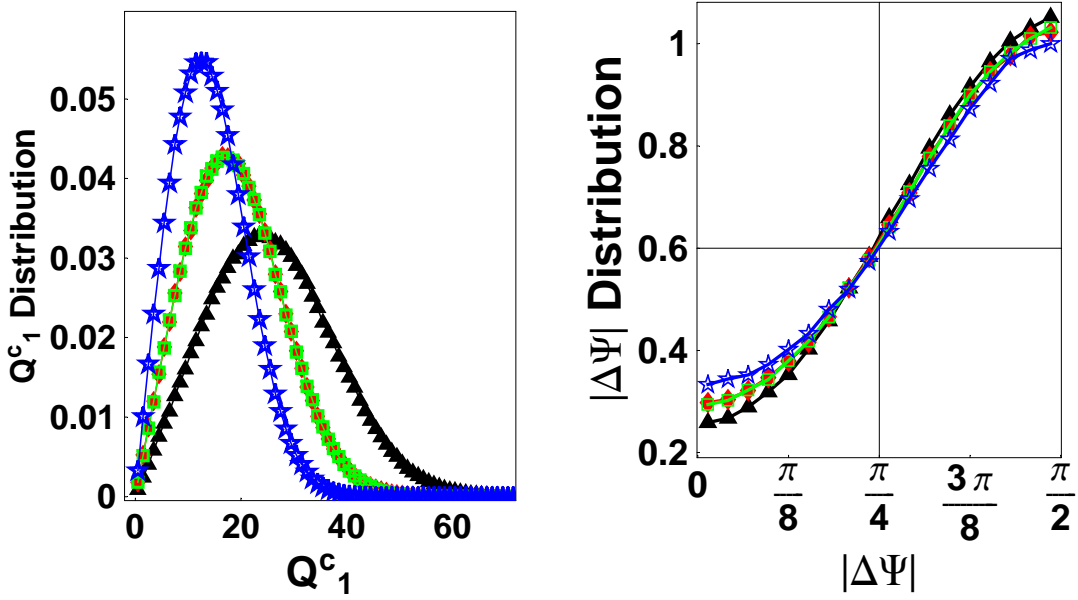


FIG. 4: The Q_1^c (left) and $|\Delta\Psi|$ (right) distributions for the four cases in Test-I. The triangle(black), diamond(red), box(green), and star(blue) symbols are for Case-IIIc, IIIc-(α), IIIc-(β), and IIIc-(γ) respectively (see text for more details).

TABLE I: Various observables in Test-I (see text).

$\langle \hat{O} \rangle$	IIIc	IIIc-(α)	IIIc-(β)	IIIc-(γ)
$\langle (Q_1^c)^2 \rangle$	799.8	437.8	437.6	253.1
$\langle (Q_2)^2 \rangle$	1998.2	2024.8	2027.9	2047.0
$\langle (\Delta Q^2) \cdot Q_2 \rangle$	-13109.4	-7345.3	-7400.1	-4314.1
$\langle \cos(\phi_i - \phi_j) \rangle_{++/--}$	0.0025	-0.00078	0.00197	-0.00131
$\langle \cos(\phi_i - \phi_j) \rangle_{+-}$	-0.0025	-0.00125	0.00149	0.00053
$\langle \cos(2\phi_i - 2\phi_j) \rangle_{++/--}$	0.0100	0.0102	0.0102	0.0103
$\langle \cos(2\phi_i - 2\phi_j) \rangle_{+-}$	0.0100	0.0102	0.0102	0.0103
$\frac{1}{v_2} \langle \cos(\phi_i + \phi_j - 2\phi_k) \rangle_{++/--, k-any}$	-0.0025	-0.00167	-0.00107	-0.00109
$\frac{1}{v_2} \langle \cos(\phi_i + \phi_j - 2\phi_k) \rangle_{+-, k-any}$	0.0025	0.00130	0.00192	0.00082
$\langle \cos(2\Delta\Psi) \rangle$	-0.3118	-0.2873	-0.2889	-0.2636

and negative charges in the out-of-plane direction, while both the SCBB and the OCSS correlations, either by separating same-charge pairs or by focusing opposite-charge pairs,

tend to reduce the out-of-plane charge separation.

B. Test-II

It is important to assess how the above features change with the magnitude of the built-in dipole. We thus also study a similar setting to Test-I but with a smaller out-of-plane dipole $d_1 = 0.02$. Again, we have four cases: **Case-IV** with the smaller dipole, and **Case-IV-(α),(β),(γ)** with the smaller dipole plus the same correlations as in the **Case-IIIc-(α),(β),(γ)**. The results are shown in Fig.5 and Table.II. The qualitative conclusion is largely the same as in Test-I, except for a few differences:

- (1) Not surprisingly the angular distribution is much flatter due to a smaller dipole, and the $\langle \cos(2 \Delta \Psi) \rangle$ is getting much closer to zero though still negative;
- (2) **Case-IV-(β)** is interesting, since one finds $\frac{1}{v_2} \langle \cos(\phi_i + \phi_j - 2\phi_k) \rangle_{++/--, k-any}$ to be *positive* although there is still out-of-plane charge separation (as indicated by angular distribution and negative $\langle \cos(2 \Delta \Psi) \rangle$).

C. Test-III

In this test we completely turn off the dipole, i.e. $d_1 = 0$, in order to expose the effects due to correlations. Here the **Case-Ib** (previously studied) has elliptic flow but no dipole and represents charge separation from pure statistical fluctuation, while **Case-Ib-(α),(β),(γ)** have no dipole but the same correlations as in the **Case-IIIc-(α),(β),(γ)**. The results are reported in Fig.6 and Table.III¹³. A comparison with Test-I,II shows the following:

- (1) The correlator $\langle \cos(\phi_i - \phi_j) \rangle$ for both same-charge and opposite charge pairs show similar patterns as before, which indicates that they are most sensitively dominated by the correlations;
- (2) Most surprisingly, we find the correlations to rotate the angular distribution in opposite direction to the previous cases;
- (3) Furthermore **Case-Ib-(γ)** (see last column of Table.III), even without a physical dipole, shows a sign pattern for all four measured charge correlations qualitatively similar to the

¹³ In Table.III and IV certain extremely small values are given in the form of $\hat{o}(10^{-n})$, which means they are consistent with zero provided our finite statistics and may exactly vanish at infinite statistics limit.

Case-IIIc-(γ) and to the STAR data.

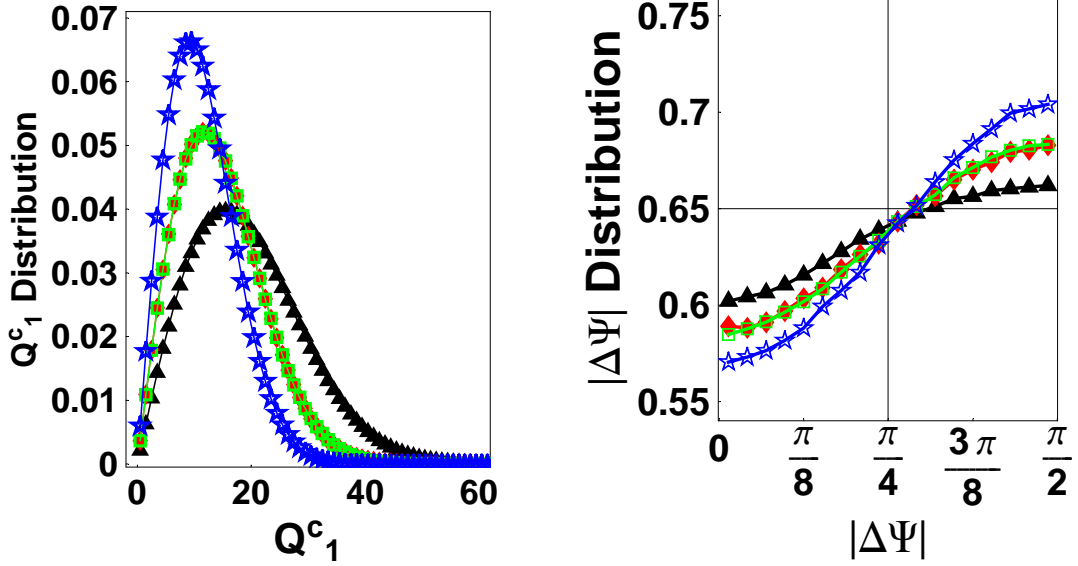


FIG. 5: The Q_1^c (left) and $|\Delta\Psi|$ (right) distributions for the four cases in Test-II. The triangle(black), diamond(red), box(green), and star(blue) symbols are for Case-IV, IV-(α), IV-(β), and IV-(γ) respectively (see text for more details).

TABLE II: Various observables in Test-II (see text).

$\langle \hat{O} \rangle$	IV	IV-(α)	IV-(β)	IV-(γ)
$\langle (Q_1^c)^2 \rangle$	464.0	269.6	269.8	166.5
$\langle (Q_2)^2 \rangle$	1996.5	2001.4	2001.7	2004.5
$\langle (\Delta Q^2) \cdot Q_2 \rangle$	-423.8	-704.1	-716.5	-719.3
$\langle \cos(\phi_i - \phi_j) \rangle_{++/--}$	0.0004	-0.00184	0.00091	-0.00185
$\langle \cos(\phi_i - \phi_j) \rangle_{+-}$	-0.0004	-0.00020	0.00253	0.00107
$\langle \cos(2\phi_i - 2\phi_j) \rangle_{++/--}$	0.0100	0.0100	0.0100	0.0101
$\langle \cos(2\phi_i - 2\phi_j) \rangle_{+-}$	0.0100	0.0100	0.0100	0.0101
$\frac{1}{v_2} \langle \cos(\phi_i + \phi_j - 2\phi_k) \rangle_{++/--, k-any}$	-0.0004	-0.00056	0.00003	-0.00049
$\frac{1}{v_2} \langle \cos(\phi_i + \phi_j - 2\phi_k) \rangle_{+-, k-any}$	0.0004	0.00021	0.00080	0.00022
$\langle \cos(2 \Delta\Psi) \rangle$	-0.0232	-0.0375	-0.0387	-0.0527

It appears that on top of the charge separations due to statistical fluctuations, the correlations studied here seem to actually suppress the in-plane separation while “enhancing”

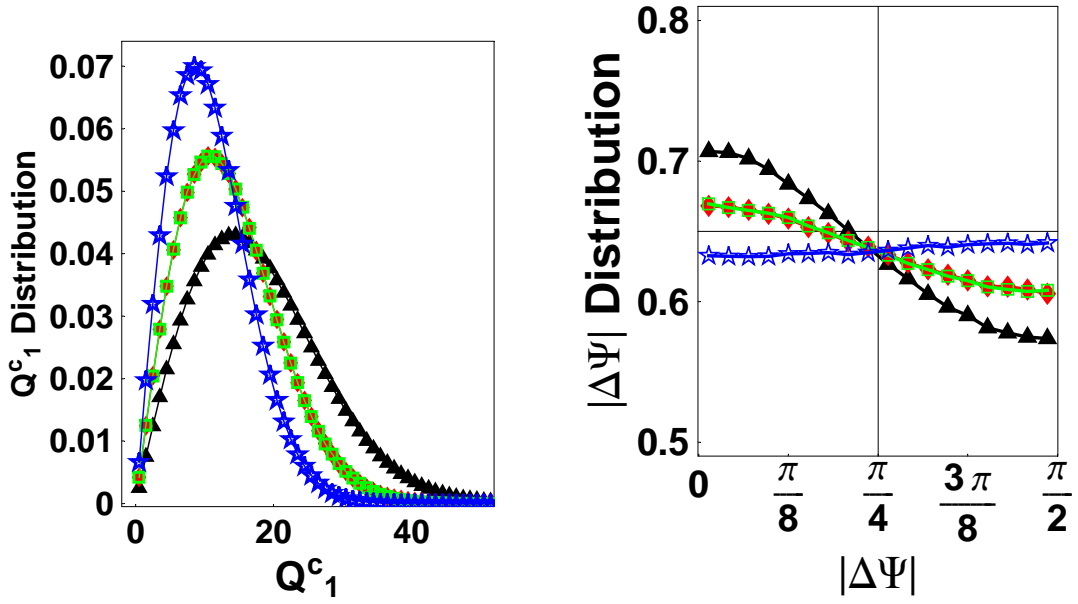


FIG. 6: The Q_1^c (left) and $|\Delta\Psi|$ (right) distributions for the four cases in Test-III. The triangle(black), diamond(red), box(green), and star(blue) symbols are for Case-Ib, Ib- (α) , Ib- (β) , and Ib- (γ) respectively (see text for more details).

TABLE III: Various observables in Test-III (see text).

$\langle \hat{o} \rangle$	Ib	Ib- (α)	Ib- (β)	Ib- (γ)
$\langle (Q_1^c)^2 \rangle$	400.1	237.8	237.7	150.0
$\langle (Q_2)^2 \rangle$	1996.7	1996.2	1995.2	1996.1
$\langle (\Delta Q^2) \cdot Q_2 \rangle$	1998.3	543.1	548.6	-56.34
$\langle \cos(\phi_i - \phi_j) \rangle_{++/--}$	$\hat{o}(10^{-7})$	-0.00204	0.00071	-0.00196
$\langle \cos(\phi_i - \phi_j) \rangle_{+-}$	$\hat{o}(10^{-7})$	$\hat{o}(10^{-7})$	0.00118	0.00053
$\langle \cos(2\phi_i - 2\phi_j) \rangle_{++/--}$	0.0100	0.0100	0.0100	0.0100
$\langle \cos(2\phi_i - 2\phi_j) \rangle_{+-}$	0.0100	0.0100	0.0100	0.0100
$\frac{1}{v_2} \langle \cos(\phi_i + \phi_j - 2\phi_k) \rangle_{++/--, k-any}$	$\hat{o}(10^{-7})$	-0.00036	0.00024	-0.00038
$\frac{1}{v_2} \langle \cos(\phi_i + \phi_j - 2\phi_k) \rangle_{+-, k-any}$	$\hat{o}(10^{-6})$	$\hat{o}(10^{-7})$	0.00059	0.00011
$\langle \cos(2\Delta\Psi) \rangle$	0.0532	0.0242	0.0245	-0.0038

the out-of-plane separation to some extent. The reason for this behavior is the presence of elliptic flow: while the two-particle correlations themselves are reaction-plane independent,

due to the elliptic flow there are (on average) more pairs close to the in-plane direction than pairs close to the out-of-plane direction. Therefore, the correlations are more effective in the in-plane direction. Since, as already discussed, the correlations considered here tend to suppress the charge separation, the *statistical* charge separations are more suppressed in-plane than out-of-plane. As a result we observe an effective “enhancement” of out-of-plane charge separation. This subtle effect is proportional to the magnitude of the elliptic flow, v_2 , and the correlation strength.

D. Test-IV

The results in Test-III suggest an interesting question: could it be that in a certain parameter region, the same out-of-plane charge separation (e.g. the same $|\Delta\Psi|$ distribution) can be produced either by a physical dipole (e.g. due to Chiral Magnetic Effect) or by any one of the SCBB or OCSS correlations? It turns out that this is possible. Here in Test-IV we provide an example:

Case-V-(α) with only a physical out-of-plane dipole $d_1 = 0.025$;

Case-V-(β) with no physical dipole and only SCBB correlation at a fraction $f_{SCBB} = 1\%$;

Case-V-(γ) with no physical dipole and only OCSS correlation at a fraction $f_{OCSS} = 1\%$.

In addition we also include the previously studied **Case-Ib** with only statistical fluctuation as a reference for comparison. The results are presented in Fig.7 and Table.IV. A few very interesting features can be immediately seen:

- (1) All three cases V-(α)(β)(γ) show almost identical $|\Delta\Psi|$ distribution and $\langle\cos(2\Delta\Psi)\rangle$, i.e. three distinctive physical effects can lead to quantitatively similar “apparent” out-of-plane charge separation;
- (2) The physical dipole in V-(α), however, shifts the Q_1^c distribution toward larger values while the correlations in V-(β)(γ) shift the distribution toward smaller values, thus making the Q_1^c distribution also an important discriminating probe;
- (3) The observable $\frac{1}{v_2}\langle\cos(\phi_i + \phi_j - 2\phi_k)\rangle$ has almost the same value in V-(α) with physical dipole and in V-(β) with SCBB correlation and thus can not distinguish the two cases, but it differentiates the V-(γ) with OCSS correlation;
- (4) The correlator $\langle\cos(\phi_i - \phi_j)\rangle$ again appears to be a sensitive observable, giving different sign patterns for the three cases.

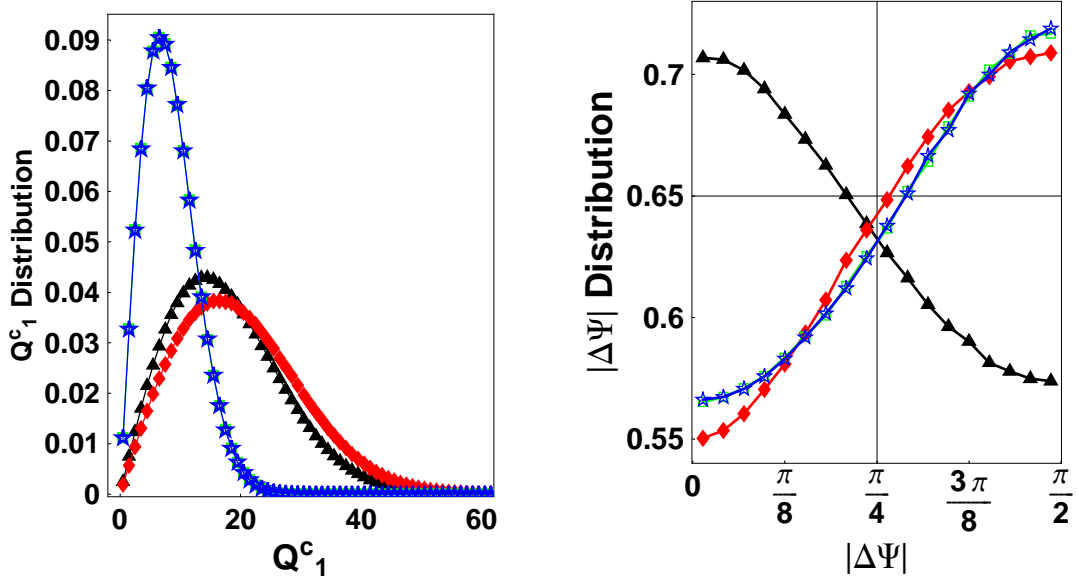


FIG. 7: The Q_1^c (left) and $|\Delta\Psi|$ (right) distributions for the four cases in Test-IV. The triangle(black), diamond(red), box(green), and star(blue) symbols are for Case-Ib, V-(α), V-(β), and V-(γ) respectively (see text for more details).

TABLE IV: Various observables in Test-IV (see text).

$\langle \hat{O} \rangle$	Ib	V-(α)	V-(β)	V-(γ)
$\langle (Q_1^c)^2 \rangle$	400.1	499.8	89.4	89.4
$\langle (Q_2)^2 \rangle$	1996.7	1995.9	1996.2	1995.8
$\langle (\Delta Q^2) \cdot Q_2 \rangle$	1998.3	-1762.9	-499.4	-497.2
$\langle \cos(\phi_i - \phi_j) \rangle_{++/--}$	$\hat{\delta}(10^{-7})$	0.00062	-0.00390	0.00733
$\langle \cos(\phi_i - \phi_j) \rangle_{+-}$	$\hat{\delta}(10^{-7})$	-0.00063	$\hat{\delta}(10^{-7})$	0.01118
$\langle \cos(2\phi_i - 2\phi_j) \rangle_{++/--}$	0.0100	0.0100	0.0100	0.0100
$\langle \cos(2\phi_i - 2\phi_j) \rangle_{+-}$	0.0100	0.0100	0.0100	0.0100
$\frac{1}{v_2} \langle \cos(\phi_i + \phi_j - 2\phi_k) \rangle_{++/--, k-any}$	$\hat{\delta}(10^{-7})$	-0.00062	-0.00059	0.00343
$\frac{1}{v_2} \langle \cos(\phi_i + \phi_j - 2\phi_k) \rangle_{+-, k-any}$	$\hat{\delta}(10^{-6})$	0.00062	$\hat{\delta}(10^{-8})$	0.00400
$\langle \cos(2\Delta\Psi) \rangle$	0.0532	-0.06243	-0.05996	-0.05994

The most important lessons we learn from these tests and especially from Test-IV are: first, the proposed $|\Delta\Psi|$ distribution and $\langle\cos(2\Delta\Psi)\rangle$ can readily reveal the geometry of any potential charge separation; second, an out-of-plane charge separation may arise due a physical out-of-plane dipole (e.g. with Chiral Magnetic Effect) or due to specific types of two-particle correlations (e.g. SCBB or OCSS); third, the unambiguous way to disentangle these different sources contributing to an out-of-plane charge separation, is to measure all the available observables including both the Q_1^c magnitude and angular distribution and the STAR observables $\frac{1}{v_2}\langle\cos(\phi_i + \phi_j - 2\phi_k)\rangle$ and $\langle\cos(\phi_i - \phi_j)\rangle$ as well.

V. SUMMARY

To summarize, in this paper we have introduced and studied a method to experimentally extract a possible charge separation in the relativistic heavy ion collisions. Specifically we have proposed to measure the event-by-event distribution of the charged dipole vector, \hat{Q}_1^c . This analysis is able to determine the magnitude of the dipole as well as its azimuthal orientation with respect to the reaction plane. Using Monte Carlo events, we have investigated the sensitivity of this method for various scenarios, including the presence of additional two-particle correlations. We have shown that the combined information of the magnitude and direction of the dipole can distinguish between effects due to certain two particle correlations and those from e.g. the chiral magnetic effect.

As in the case of the elliptic flow analysis, the proposed method may be refined by studying the \hat{Q}_1^c distribution differentially in transverse momentum or rapidity. Further improvements may introduce transverse momentum or rapidity dependent weight factors in the \hat{Q}_1^c extraction via Eq.(11).

To conclude, we have demonstrated that our proposed method provides additional discrimination power over already existing measurements. This is essential in order to definitively determine the presence of local parity violation in heavy ion collisions.

Appendix A

In this Appendix we show some details related to the charged dipole vector \hat{Q}_1^c analysis and discuss its relation to various charged particle correlations.

The magnitude of Q_1^c itself involves a square-root and, therefore, contains all multi-particle correlations, as is evident from a Taylor expansion:

$$Q_1^c = \sqrt{N_{ch} + \{i, j\}_1^c} = N_{ch}^{\frac{1}{2}} \left[1 + \frac{1}{2N_{ch}} \{i, j\}_1^c - \frac{1}{8N_{ch}^2} (\{i, j\}_1^c)^2 + \dots \right] \quad (\text{A1})$$

with $\{i, j\}_1^c \equiv \sum_{i \neq j} q_i q_j \cos(\phi_i - \phi_j)$. For example, the third term $(\{i, j\}_1^c)^2$ in the above expansion involves 2,3,4-particle correlations. This can be explicitly evaluated to give:

$$\begin{aligned} (\{i, j\}_1^c)^2 &= N_{ch}(N_{ch} - 1) \\ &+ 2 \sum_{i \neq j} \cos(\phi_i - \phi_j) + \sum_{i \neq j} \cos 2(\phi_i - \phi_j) \\ &+ 2 \sum_{i \neq j \neq k} q_i q_j \cos(\phi_i + \phi_j - 2\phi_k) \\ &+ \sum_{i \neq j \neq k \neq l} q_i q_j q_k q_l \cos(\phi_i + \phi_j - \phi_k - \phi_l) \end{aligned} \quad (\text{A2})$$

We notice that the 3-particle correlation term in the above is precisely the one proposed in [18] and measured in [17]. However, a full \hat{Q}_1^c analysis reveals more information than those expressed by the two and three particle distributions. First, the expression for the magnitude of \hat{Q}_1^c , Eq.(A1), involves higher order terms than Eq.(A2). Thus it involves correlations beyond three particles. Second, the determination of the magnitude and azimuthal orientation of \hat{Q}_1^c necessarily involves all particles in an event and hence correlations involving more than three particles. Third, knowing the magnitude distribution of \hat{Q}_1^c allows to calculate the average of any moment $\langle (Q_1^c)^n \rangle$, which contains n-particle correlations. As discussed in [28][29] in general the average of the n -th moment of an extensive observable like Q_1^c will necessarily involve n -particle correlations.

As an example, from the definition of \hat{Q}_1^c , Eq.(11), one can calculate the 2^{nd} moment:

$$\begin{aligned} (Q_1^c)^2 &= \sum_i q_i^2 (\cos^2 \phi_i + \sin^2 \phi_i) + \sum_{i \neq j} q_i q_j (\cos \phi_i \cos \phi_j + \sin \phi_i \sin \phi_j) \\ &= N_{ch} + \sum_{i \neq j} q_i q_j \cos(\phi_i - \phi_j) \end{aligned} \quad (\text{A3})$$

which is directly related to two particle azimuthal correlations for both same-charge and opposite-charge pairs. This relation is in analogy to the familiar relation for elliptic flow, i.e.

$$(Q_2)^2 = N_{ch} + \sum_{i \neq j} \cos(2\phi_i - 2\phi_j) \quad (\text{A4})$$

Next we derive Eq.(13). We first evaluate the quantity

$$(\Delta Q^2) \cdot Q_2 \equiv [(Q_1^c)^2 \cdot \cos(2\Delta\Psi)] \cdot Q_2 \quad (\text{A5})$$

by using the definitions in Eq.(11,12):

$$\begin{aligned} [(Q_1^c)^2 \cdot \cos(2\Delta\Psi)] \cdot Q_2 &= [(Q_1^c)^2 \cos(2\Psi_1)] \cdot [Q_2 \cos(2\Psi_2)] \\ &\quad + [(Q_1^c)^2 \sin(2\Psi_1)] \cdot [Q_2 \sin(2\Psi_2)] \\ &= N_{ch} + 2 \sum_{i \neq j} q_i q_j \cos(\phi_i - \phi_j) \\ &\quad + \sum_{i \neq j} \cos 2(\phi_i - \phi_j) + \sum_{i \neq j \neq k} q_i q_j \cos(\phi_i + \phi_j - 2\phi_k) \end{aligned} \quad (\text{A6})$$

Combining the above with Eq.(A3,A4), we obtain

$$\begin{aligned} \cos(2\Delta\Psi) &= \frac{[(Q_1^c)^2 \cdot \cos(2\Delta\Psi)] \cdot Q_2}{(Q_1^c)^2 [(Q_2)^2]^{1/2}} \\ &= \frac{N_{ch} + 2 \{i, j\}_1^c + \{i, j\}_2 + \{i, j, k\}^c}{[N_{ch} + \{i, j\}_1^c] \cdot [N_{ch} + \{i, j\}_2]^{1/2}} \end{aligned} \quad (\text{A7})$$

with the two- and three- particle correlations $\{i, j\}_1^c$, $\{i, j\}_2$, $\{i, j, k\}^c$ defined in Eq.(14). The Eq.(13) is simply the event averaged version of the above expression.

Acknowledgements

The authors are indebted to A. Poskanzer for very helpful discussions. The authors also thank D. Kharzeev, R. Lacey, L. McLerran, E. Shuryak, S. Voloshin, F. Wang, and N. Xu for discussions and communications. This work was supported in part by the Director, Office of Energy Research, Office of High Energy and Nuclear Physics, Divisions of Nuclear Physics, of the U.S. Department of Energy under Contract No. DE-AC02-05CH11231. A.B. is also

supported by the Polish Ministry of Science and Higher Education, grant No. N202 125437 and the Foundation for Polish Science (KOLUMB program).

- [1] G. 't Hooft, arXiv:hep-th/0010225.
- [2] T. Schafer and E. V. Shuryak, Rev. Mod. Phys. **70**, 323 (1998).
- [3] E. Shuryak, “*The QCD Vacuum, Hadrons and Superdense Matter*”, 2nd ed., World Scientific Publishing Company, 2004.
- [4] G. Ripka, arXiv:hep-ph/0310102.
- [5] G. S. Bali, arXiv:hep-ph/9809351.
- [6] J. Greensite, Prog. Part. Nucl. Phys. **51**, 1 (2003).
- [7] J. Liao and E. Shuryak, Phys. Rev. C **75**, 054907 (2007); Phys. Rev. Lett. **101**, 162302 (2008). M. N. Chernodub and V. I. Zakharov, Phys. Rev. Lett. **98**, 082002 (2007). A. D’Alessandro and M. D’Elia, Nucl. Phys. B **799**, 241 (2008). M. Cristoforetti and E. Shuryak, Phys. Rev. D **80**, 054013 (2009) [arXiv:0906.2019 [hep-ph]]. A. D’Alessandro, M. D’Elia and E. Shuryak, arXiv:1002.4161 [hep-lat].
- [8] J. Liao and E. Shuryak, Phys. Rev. C **77**, 064905 (2008); Phys. Rev. D **73**, 014509 (2006); Nucl. Phys. A **775**, 224 (2006).
- [9] E. Shuryak, Prog. Part. Nucl. Phys. **62**, 48 (2009). D. E. Kharzeev, Nucl. Phys. A **827**, 118C (2009) [arXiv:0902.2749 [hep-ph]].
- [10] J. Liao and E. Shuryak, Phys. Rev. Lett. **102**, 202302 (2009). E. Shuryak, Phys. Rev. C **80**, 054908 (2009) [Erratum-ibid. C **80**, 069902 (2009)]. C. Ratti and E. Shuryak, Phys. Rev. D **80**, 034004 (2009). M. Lublinsky, C. Ratti and E. Shuryak, Phys. Rev. D **81**, 014008 (2010). D. M. Ostrovsky, G. W. Carter and E. V. Shuryak, Phys. Rev. D **66**, 036004 (2002).
- [11] D. Kharzeev, Phys. Lett. B **633**, 260 (2006).
- [12] D. Kharzeev and A. Zhitnitsky, Nucl. Phys. A **797**, 67 (2007).
- [13] D. E. Kharzeev, L. D. McLerran and H. J. Warringa, Nucl. Phys. A **803**, 227 (2008).
- [14] K. Fukushima, D. E. Kharzeev and H. J. Warringa, Phys. Rev. D **78**, 074033 (2008); arXiv:0912.2961 [hep-ph]; arXiv:1002.2495 [hep-ph]. D. E. Kharzeev and H. J. Warringa, Phys. Rev. D **80**, 034028 (2009).
- [15] P. V. Buividovich, M. N. Chernodub, E. V. Luschevskaya and M. I. Polikarpov, Phys. Rev.

- D **80**, 054503 (2009). P. V. Buividovich, M. N. Chernodub, E. V. Luschevskaya and M. I. Polikarpov, Nucl. Phys. B **826**, 313 (2010).
- [16] D. E. Kharzeev, Annals Phys. **325**, 205 (2010).
- [17] B. I. Abelev *et al.* [STAR Collaboration], Phys. Rev. Lett. **103**, 251601 (2009); arXiv:0909.1717 [nucl-ex].
- [18] S. A. Voloshin, Phys. Rev. C **70**, 057901 (2004).
- [19] A. Bzdak, V. Koch and J. Liao, Phys. Rev. C **81**, 031901 (2010) [arXiv:0912.5050 [nucl-th]].
- [20] F. Wang, arXiv:0911.1482 [nucl-ex].
- [21] S. Pratt, arXiv:1002.1758 [nucl-th].
- [22] R. Millo and E. Shuryak, arXiv:0912.4894 [hep-ph].
- [23] K. Fukushima, D. E. Kharzeev and H. J. Warringa, arXiv:1002.2495 [hep-ph].
- [24] G. Basar, G. V. Dunne and D. E. Kharzeev, arXiv:1003.3464 [hep-ph].
- [25] S. A. Voloshin, A. M. Poskanzer and R. Snellings, arXiv:0809.2949 [nucl-ex].
- [26] A. M. Poskanzer and S. A. Voloshin, Phys. Rev. C **58**, 1671 (1998) [arXiv:nucl-ex/9805001].
- [27] R. Lacey, “Local parity violation studies with PHENIX”, talk at the “Workshop on P- and CP-odd Effects in Hot and Dense Matter”, <http://www.bnl.gov/riken/hdm/>.
- [28] V. Koch, arXiv:0810.2520 [nucl-th].
- [29] A. Bialas and V. Koch, Phys. Lett. B **456**, 1 (1999).